Trace Analyzer

EE Circle

October, 2007

Contents

Preface

Transmission line has long been an important subject for microwave and RF engineers. With the advancement in digital technologies, especially when the clock and/or data rate reached multiple gigahertz (GHz), designers of printed circuit board (PCB) and package have to care about the parameters like trace impedance in order to maintain the signal integrity (SI). The need for transmission line parameters of the traces rises steadily.

Simple traces, such as single micro-strip, stripline and coplanar waveguide structures, can be modeled empirical formulas [1] with reasonable accuracy. However, the validity of the empirical formulas is subject to some constraints on the original geometric parameters due to the fact that they were derived from curve-fittings. Furthermore, real world engineering problems involve multiple traces in a layered dielectric media. To solve practical engineering trace design problems, the tool has to be built based on solving Maxwell's equations for 2D geometry. The topic of multiconductor transmission line (MTL) [2] was once a very active research area in the 1990's. Some of the mature methods are adopted in developing the current tool – Trace Analyzer.

CONTENTS — MANUSCRIPT

This document is split into two parts. The first part is a user's guide for Trace Analyzer, which is essential for anyone to learn how to use the tool. The second part provides under-the-hood theoretical details of the tool for the inquisitive users, which might also be useful to the advanced readers to develop their own MTL solvers.

Major feature of Trace Analyzer include:

- Integrated Material Editor
- Integrated Layer Stackup (Metal and Dielectric Layer) Editor
- Accommodating layered media with any number of dielectric/metal layers
- Designations of some metal layers to be connected to the ground (GND)
- Allowing any number of traces on any metal layers (except GND layers) with customized width and spacing rules
- Calculations of RLGC matrices and the derived impedance matrix
- Export RLGC parameters to W-element files compatible with HSPICE
- Export RLGC parameters to model file compatible with ADS
- File formats for storing material, layer stackup and trace design information

Part I

User's Guide

Chapter 1

Acknowledgement

- Trace Analyzer is written 100% in Java.
- The following Java numerical packages are instrumental building blocks is Trace Analyzer
  - Colt: a free Java toolkit at CERN for high performance computing. URL: http://dsd.lbl.gov/~hoschek/colt/
  - JAMA (JAva MAtrix package): containss common matrix routines. URL: http://math.nist.gov/javanumerics/jama/
  - Jampack (JAva Matrix PACKage): matrix solver for complex matrices. URL: ftp://math.nist.gov/pub/Jampack/Jampack/AboutJampack.html
- This document is prepared with LaTeX

Chapter 2

Typical Work Flow

Figure 2.1 is a diagram showing the work flow of typical usage of Trace Analyzer. First, the user needs to work establish a suitable layer stackup by defining the materials, dielectric and metal layers. Next, traces can be added by specifying the width and position coordinates. The collection of traces constitutes a MTL system, which can be solved for its R/L/G/C matrices. Information of the layer stackup and traces can be stored into separate files, such that they are reusable. Results of the RLGC matrices can be stored in one of the standard file formats usaed by commercial simulation tools like HSPICE and ADS. A specific design is captured by a Trace Analyzer project file, which merely points to a layer stackup file, a trace file, and optionally an RLGC file.

Remark 1 A project file stores a few lines of file names for the layer stackup, traces, and (optionally) RLGC. The file names do not contain absolute directory names for

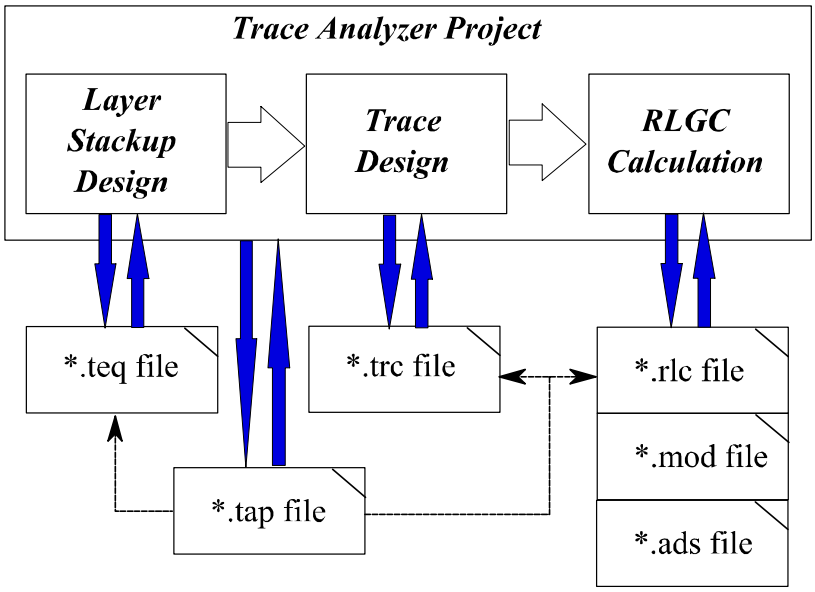

Figure 2.1: Typical work flow of using Trace Analyzer.

maximum portability. As a consequence, the layer stackup, traces, and RLGC files should always reside in the same directory as the project file. User may need to make copies when a stackup/trace file is shared by multiple projects.

Chapter 3

Modules of Trace Analyzer

Trace Analyzer, at the to-level, is composed of three major GUI parts: Menu bar, Main panel and Message area as shown in Figure 3.1. The menu items under Menu bar are:

- Project
  - New: start a new project. Any existing information about layer stackup, trace and RLGC will be flushed away.
  - Open: open an existing project file.
  - Save: update an existing project file with the latest modification.
  - Save As: save the current design information to a new project file.
  - Exit: exit the tool.
- Stackup

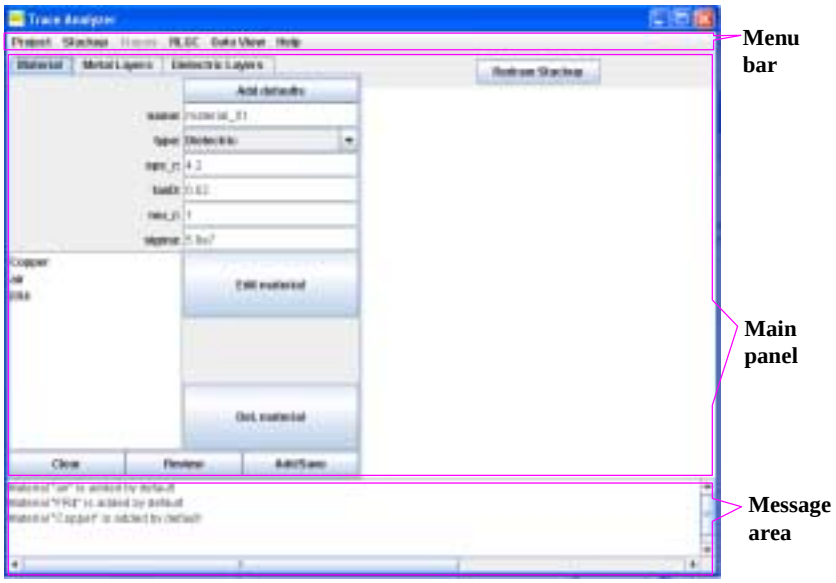

Figure 3.1: Trace Analyzer Top-level parts.

– Set Z Unit: The Z direction is perpendicular to all metal/dielectric layers. User can choose a convenient unit, such as mm, mil, and um.

– New Stackup: start a new layer stackup design. Any existing layer stackup information will be flushed away.

– Open Stackup: open an existing layer stackup file.

– Save Stackup: update an existing layer stackup file with the latest definitions.

– Save Stackup As: save the current layer stackup information to a new layer stackup file.

- Traces

  - Set X Unit: The X direction is the one-dimensional coordinate system for trace position, width, spacing and etc.. User can choose the easiest unit suitable for the design.
  - New Traces: start a new composition of traces. Any existing trace definitions will be thrown away.
  - Open Traces: open trace design from an existing trace file.
  - Save Traces: update an existing trace file with the latest trace designs.
  - Save Traces As: save the current trace information to a new trace file.
  - Set Grounding Traces: allow user to specify some of the traces to be grounded. This is essential for analyzing the coplanar waveguide (CPW) structures.
  - No Grounding Traces: remove all the grounding designations from traces.

- RLGC
  - Calculate RLGC: start computations for R/L/G/C matrices.
  - Export RLGC for HSPICE: export RLGC file accepted by HSPICE.
  - Export W-Model for HSPICE: export RLGC model (another flavor) file accepted by HSPICE.
  - Export RLGC for ADS: export RLGC results to a file usable by ADS.

- Goto View: manually toggle between the following modules

  - Stackup
  - Traces
  - Results

- Help
  - About: display the software and user license information.

Figure 3.2: The Material Editor module.

3.1 Material Editor

The Material Editor shown in Figure 3.2 provides support for composing materials used in the design. Typical actions required can be addressed through the appropriate sequences:

- Defining a new material
  - enter a new name in the "name:" text field;
  - choose "type:" to be either Dielectric or Metal;
  - enter a value for "eps_r" (required only for Dielectric type), the relative dielectric constant;

  - enter a value for "tanD" (required only for Dielectric type), the dielectric loss tangent;
  - enter a value for "mu_r" (not used in the current version), the relative permeability;
  - enter a value for "sigma" (required only for Metal type), the conductivity;
  - click the "Add/Save" button. The newly added material should appear in the list.

- Modifying an existing material
  - select the material name from the list;
  - click the "Edit Material" button. All the text fields will be updated with the selected material properties;
  - make changes to any fields of interests;
  - click the "Add/Save" button.

3.2 Layer Stackup Editor

Layer stackup is a technical jargon used by the designers of printed circuit boards (PCBs) or packages. It specifies how the dielectric layers are stacked, and how the metal layers are sandwiched between the dielectric layers. The following essential assumptions are very important to the user:

- A stackup is always implicitly terminated by one air (or vacuum) layer of infinite thickness on the top-most dielectric layer, and one air layer of infinite thickness below the bottom-most dielectric layer.
- Conceptually, dielectric layers are introduced first.
- Conceptually, metal layers are anchored at the interior boundaries between adjacent dielectric layers.
  - No metal layer can be defined on the exterior boundaries of top-air and bottom-air boundaries.
- There are always (N+1) dielectric layer for N metal layers.
  - User can define the number of metal layers first to be Nm (insides the Metal Layer Editor). Then, the number of dielectric layers will be automatically set to (Nm+1);
  - User can also define the number of dielectric layers first to be Nd (insides the Dielectric Layer Editor). Then, the number of metal layers will be automatically set to (Nd-1);
- At each dielectric layer boundary, when the "is plane" flag turned off, a metal layer normally is immersed into either of the abutting dielectric layer, which can take position of either "below" or "above" the boundary. A special position of

the metal layer is assigned by setting the "is plane" flag turned on to indicate that the entire metal layer is inserted.

- Metal/dielectric layers are indexed from 1 at the top and increasing toward the bottom.

The overall layer stackup editing capabilities are realized by the Metal Layer Editor and the Dielectric Layer Editor.

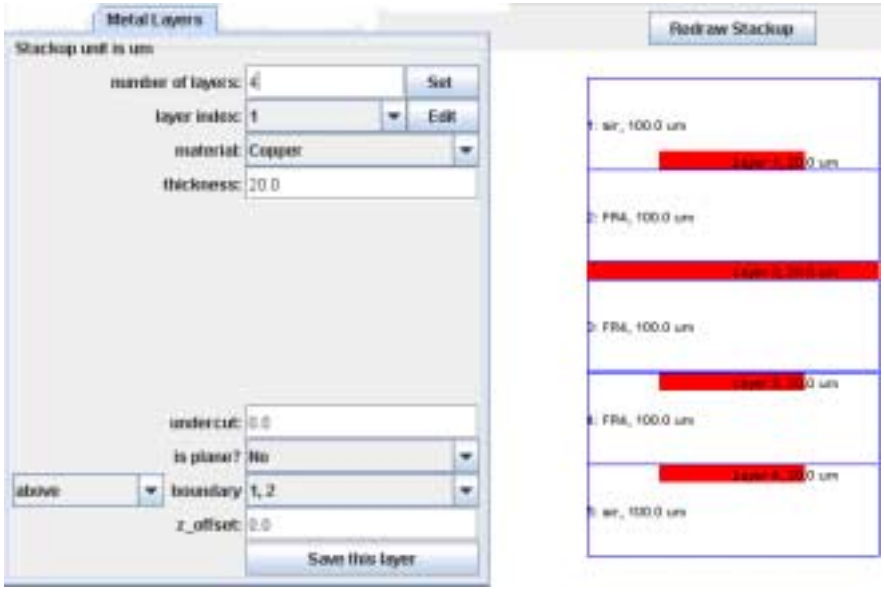

Figure 3.3: Metal Layer Editor Module.

3.2.1 Metal Layer Editor

The Metal Layer Editor shown in Figure 3.3 facilitates the following common tasks:

- Set number of metal layers
  - simply fill in the text field “number of layers:” with the desired number, then click the ”Set” button.
- Set metal layer attributes
  - choose the “layer index” from drop-down list;
  - optionally, click button “Edit” to load the stored attributes associated with this layer;

- choose a “material:” name based on available metal materials;
- set “thickness” using the current Z-unit. User can double check the Z-unit by invoking menu “Stackup::Set Z Unit”;
- the “undercut:” field is currently not used;
- set the “is plane?” flag;
- set the “above/below” choice;
- the “z_offset” is currently not used;
- click the “Save this layer” button to update.

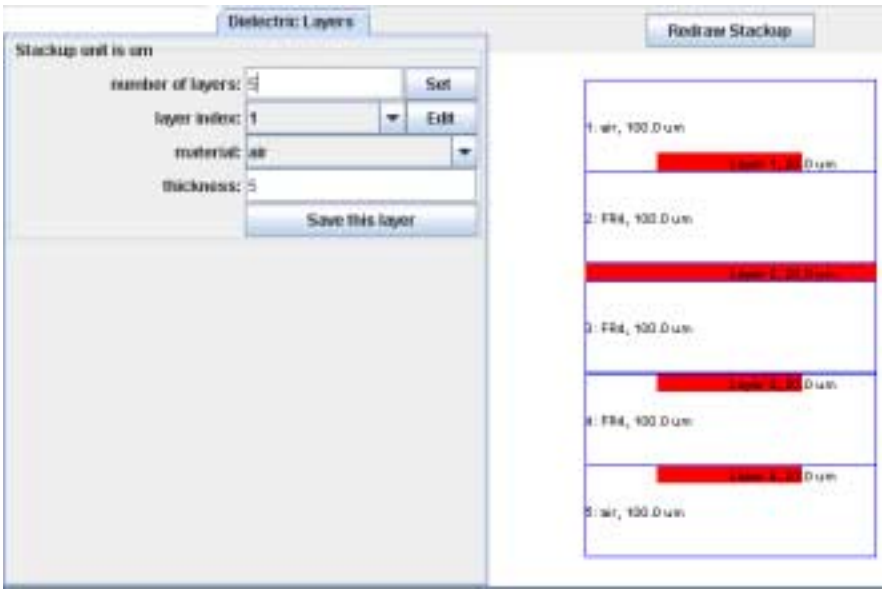

Figure 3.4: The Dielectric Layer Editor Module.

3.2.2 Dielectric Layer Editor

The Dielectric Layer Editor shown in Figure 3.4 facilitates the following common tasks:

- Set number of dielectric layers
  - simply fill in the text field “number of layers:” with the desired number, then click the ”Set” button.
- Set dielectric layer attributes
  - choose the “layer index” from drop-down list;
  - optionally, click button “Edit” to load the stored attributes associated with this layer;

– choose a “material:” name based on available metal materials;

– set “thickness” using the current Z-unit. User can double check the Z-unit by invoking menu “Stackup::Set Z Unit”;

– click the “Save this layer” button to update.

Figure 3.5: The Trace Editor Module.

3.3 Trace Editor

The Trace Editor shown in Figure 3.5 is designed to minimize the user effort in specifying the trace geometry information. There are a few conventions and operations that the user should be familiar with:

- Each trace is fully specified by
  - the metal layer index;
  - the X-coordinate of the left edge, which is labeled immediately below the trace;

  - trace width, which is labeled immediately above the trace.

- The text field after "width" specifies the next trace width.

- The text field after "left edge coordinate:" is assigned to the Xin variable.

- The tool always keeps an X-REFERENCE value (which is 0 initially);

  - X-REFERENCE assigned to be the right edge of the latest added trace.

- User can toggle between two coordinate modes by clicking the appropriate radio button:

  - in the "relative to the right edge of last trace" mode, the new trace left edge coordinate is X = Xin + X-REFERENCE;

  - in the "absolute" mode, the new trace left edge coordinate is X = Xin.

- A click on the "Add" button will add a new trace.

- A click on the "Remove Last Trace" will remove the last added trace.

- To start a new design, use menu item "Traces::New Trace".

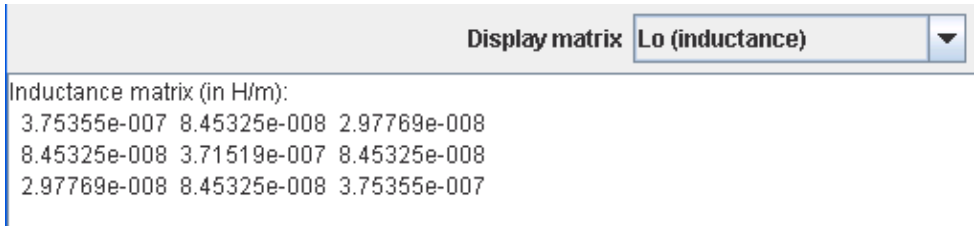

Figure 3.6: Result Viewer Module.

3.4 Result Viewer

Upon the completion of the RLGC calculation, the results can be immediately displayed for visual inspection. As shown Figure 3.6, a drop-down list can be used to choose reporting of one of the following parameters:

- Lo: inductance matrix;
- Co: capacitance matrix;
- Ro: DC resistance matrix;
- Rs: skin-effect resistance matrix;
- Gd: AC conductance matrix;
- per-unit-length delay;
- phase velocity;
- characteristic impedance.

Chapter 4

Bench Marks

To ensure the accuracy of the tool, some bench mark cases have been developed. In most applications, the L and C matrices are the most important parameters. To minimize complications, the characteristic impedances under lossless condition (or equivalently letting frequency to approach infinity while ignoring Gd), by setting R's and G's to zeros, are used for comparison. At least one other established MTL tools are used to solve the same problem with impedance number tabulated. In those cases, the relative differences of impedance values generated by Trace Analyzer are less than 3%.

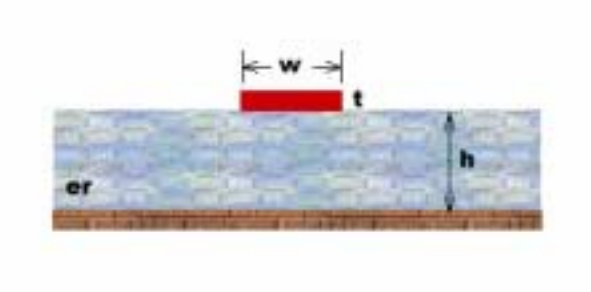

Figure 4.1: Bench mark case of single microstrip.

4.1 Single Microstrip

The parameters for the microstrip are given below:

- w = 10 mil
- t = 2.8 mil
- h = 8 mil
- er = 5.23

Characteristic impedance values from measurement [3], and LINPAR [4], a method of moment (MOM) tool, are listed below:

Method	**Z0 (ohm)**
measurement	53
LINPAR	53.82
Trace Analyzer	53.55

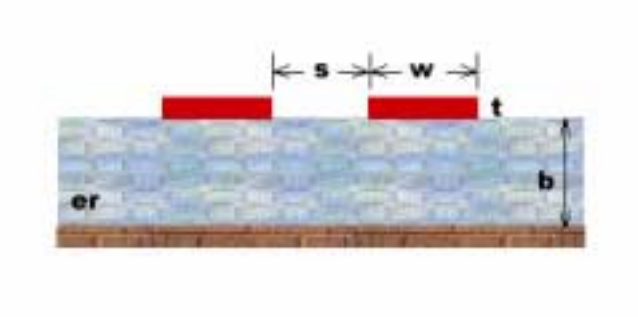

Figure 4.2: Bench mark case of two coupled microstrips.

4.2 Coupled Microstrip

The parameters for the two microstrips are given below:

- w = 10 mil
- s = 5 mil
- t = 2.8 mil
- h = 8 mil
- er = 5.23

Characteristic impedance values from measurement, and LINPAR, a method of moment (MOM) tool, are listed below:

Method	**Zodd (ohm)**	**Zeven (ohm)**
LINPAR	38.47	65.67
Trace Analyzer	38.41	65.31

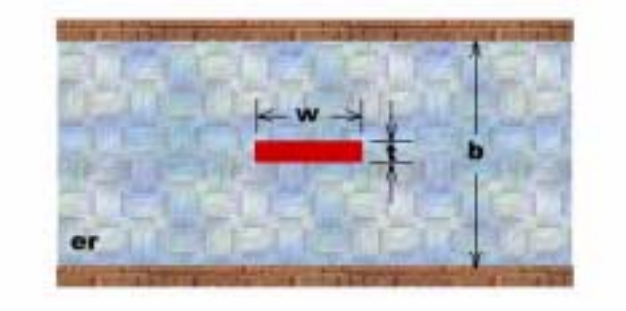

Figure 4.3: Bench mark case of single stripline.

4.3 Single Stripline

The parameters for the stripline are given below:

- w = 12.5 um
- b = 25.4 um
- t = 1.4 um
- er = 3.25

The characteristic impedance values computed by FlexPDE [5] (pp. 242-243), a finite element (FEM) tool, and LINPAR, a method of moment (MOM) tool, are listed below:

Method	**Z0 (ohm)**
FlexPDE	50
LINPAR	49.59
Trace Analyzer	49.05

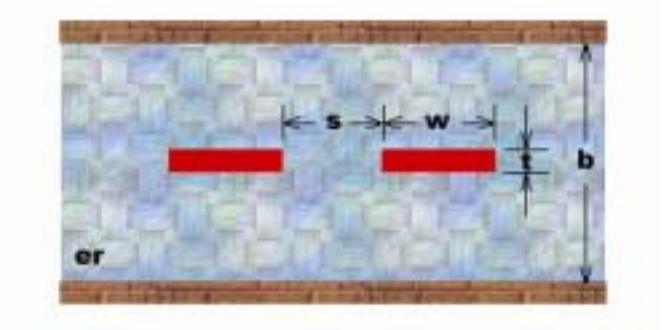

Figure 4.4: Bench mark case of two coupled striplines.

4.4 Coupled Stripline

The parameters for the coupled striplines are given below:

- w = 11.7 um
- s = 6.4 um
- b = 25.4 um
- t = 1.4 um
- er = 3.25

Characteristic impedance values computed by FlexPDE [5] (pp. 246-248), a finite element (FEM) tool, and LINPAR, a method of moment (MOM) tool, are listed below:

Method	**Zodd (ohm)**	**Zeven (ohm)**
FlexPDE	41.05	60.56
LINPAR	40.82	59.75
Trace Analyzer	40.94	60.40

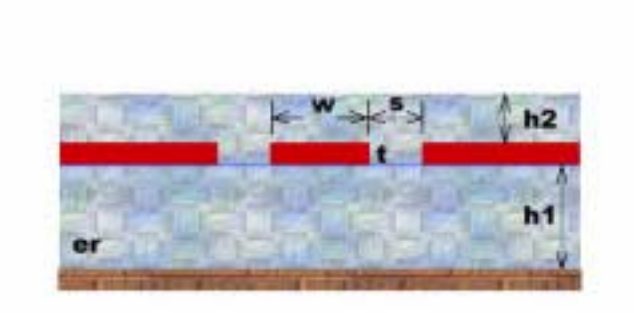

Figure 4.5: Bench mark case of ground backed coplanar waveguide with dielectric overlay.

4.5 Ground Backed CPW with Dielectric Overlay

The above structure has dielectric overlay which doesn't fit into the standard template of many solvers, but it is easily handled by Trace Analyzer. The parameters for the stripline are given below:

- w = {30, 60} mil
- s = 15 mil
- t = 0 mil (2 mil is used in Trace Analyzer)
- h1 = 42 mil
- h2 = 20 mil

- er = 4.4

Characteristic impedance value computed by QuickField [5] (pp. 250-251), a finite element (FEM) tool is listed below:

Method	**Zodd (ohm)**	**Zeven (ohm)**
QuickField	49.26	38.97
Trace Analyzer	50.58	40.11

Chapter 5

Examples

The benchmark results in the previous chapter illustrated the accuracy this tool may provide. More practical examples are shown in this chapter to analyze traces used in various realistic substrate environment such as PCB, package, and thin-film designs. With the popularity of differential signaling in higher speed operations, more than half of the examples try to target a differential impedance about 100 ohm. These project files reside in the example sub-directory of the program distribution.

5.1 Broad-side Coupled Coplanar Lines

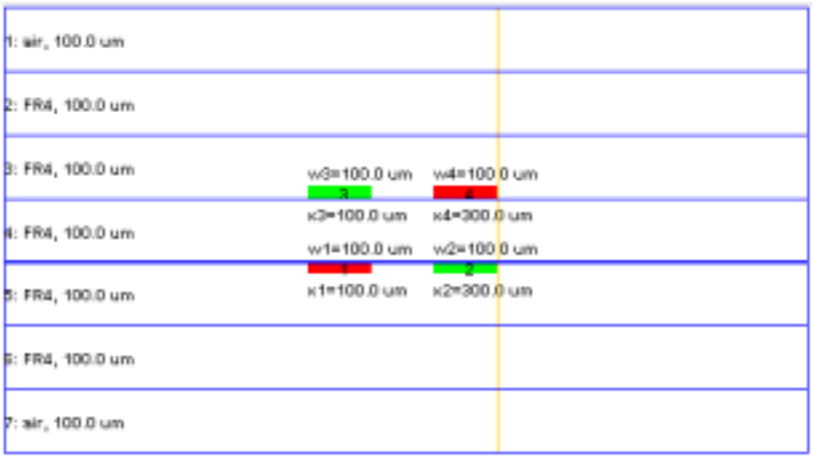

Figure 5.1: Broad-side coupled co-planar waveguide structure.

Four PCB traces are routed on two adjacent metal layers as shown in Figure 5.1. The dielectric constant is 4.2. Two of the traces are grounded, results in a coplanar transmission-line in each layer. Due to the proximity of the traces, the two sets of the coplanar lines are strongly coupled. The resultant impedance matrix is shown in Figure 5.2. This project file is under /examples/bc_cpw.

```
Characteristic impedance in (Ohm), ignoring losses:
 5.97810e+001  7.00171e+000
 7.00171e+000  5.97755e+001
```

Figure 5.2: Impedance matrix of the broad-side coupled co-planar traces.

5.2 Shielded PCB Traces

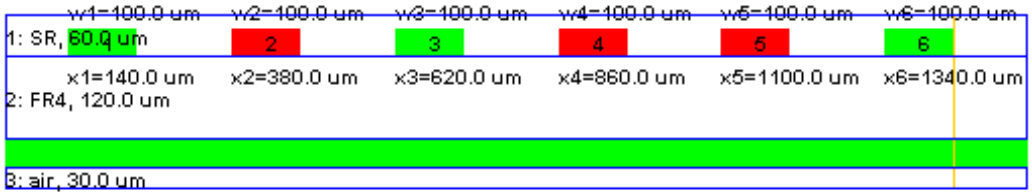

Figure 5.3: PCB traces with guard/shielding traces.

Six PCB traces are laid out on a microstrip layer as shown in Figure 5.3. Three of the lines are tied to ground, resulting in a single-ended trace and a pair of differential signal traces. The coupling effect between the single-ended and differential traces are reflected in the final impedance matrix in Figure 5.4. This project file is under /examples/pcb_shield.

Characteristic impedance in (Ohm), ignoring losses:

5.70157e+001	9.78157e-001	5.49578e-001
9.78157e-001	5.90943e+001	1.11431e+001
5.49578e-001	1.11431e+001	5.91054e+001

Figure 5.4: Impedance matrix of system including a single-ended signal and a pair of differential signal traces (with ground guards).

5.3 Coupled Striplines in PCB

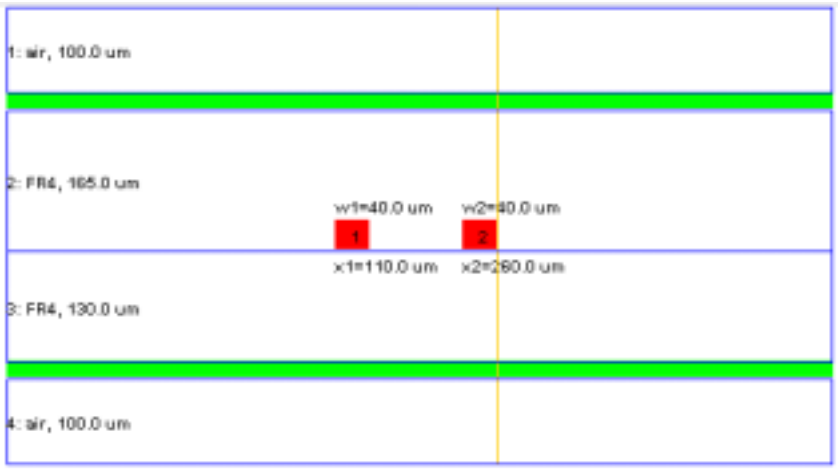

Figure 5.5: Coupled striplines in a PCB structure.

A pair of traces are routed in a PCB stripline layer as shown in Figure 5.5. The trace widths are 40 um, with spacing of 110 um. The resultant impedance matrix is shown in Figure 5.6. This project file is under /examples/pcb_stripline2.

Characteristic impedance in (Ohm), ignoring losses:
Even mode: 7.46766e+001, Common mode: 3.73383e+001
Odd mode: 4.96680e+001, Differential mode: 9.93361e+001

Figure 5.6: Impedance matrix of the coupled striplines in a PCB structure.

5.4 Coupled Microstrips in PCB

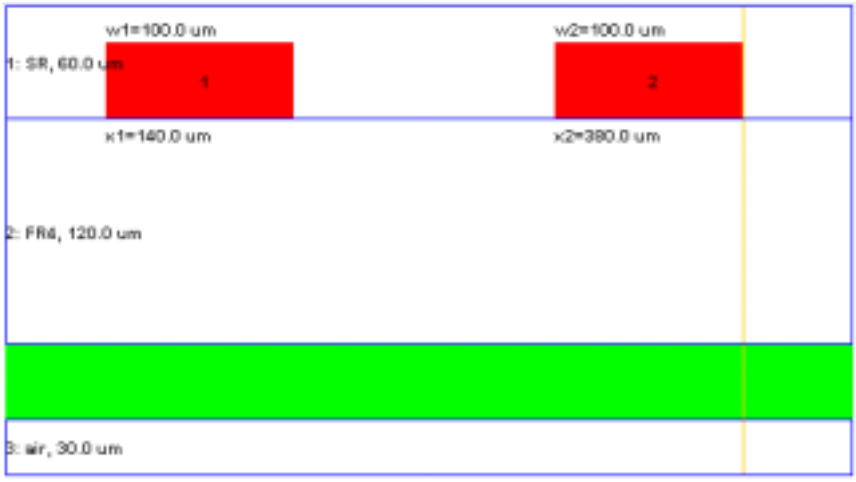

Figure 5.7: Coupled microstrips in a PCB layer.

Two coupled microstrips are laid in a PCB structure as shown in Figure 5.7. The trace widths are 100 um, with spacing of 140 um. The calculated impedance matrix is shown in Figure 5.8. This project file is under /examples/pcb_ustrip2.

```
Characteristic impedance in (Ohm), ignoring losses:
 Even mode: 7.57184e+001, Common mode: 3.78592e+001
 Odd mode: 4.96648e+001, Differential mode: 9.93295e+001
```

Figure 5.8: Impedance matrix of a pair of coupled microstrips in a PCB environment.

5.5 Coupled Striplines in Package

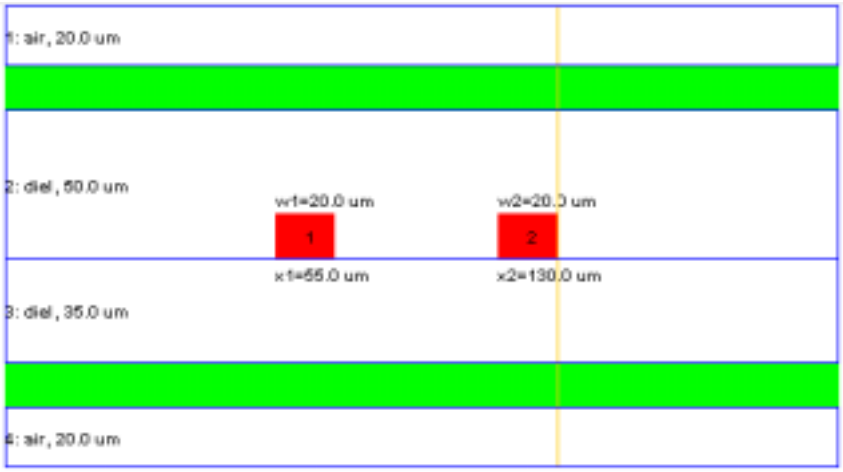

Figure 5.9: Coupled striplines in a package structure.

A pair of traces are routed in a package stripline layer as shown in Figure 5.9. The trace widths are 20 um, with spacing of 55 um. The resultant impedance matrix is shown in Figure 5.10. This project file is under /examples/pkg_stripline2.

Characteristic impedance in (Ohm), ignoring losses:
Even mode: 5.93005e+001, Common mode: 2.96503e+001
Odd mode: 4.95556e+001, Differential mode: 9.91112e+001

Figure 5.10: Impedance matrix of the coupled striplines in a package structure.

5.6 Coupled Microstrips in Package

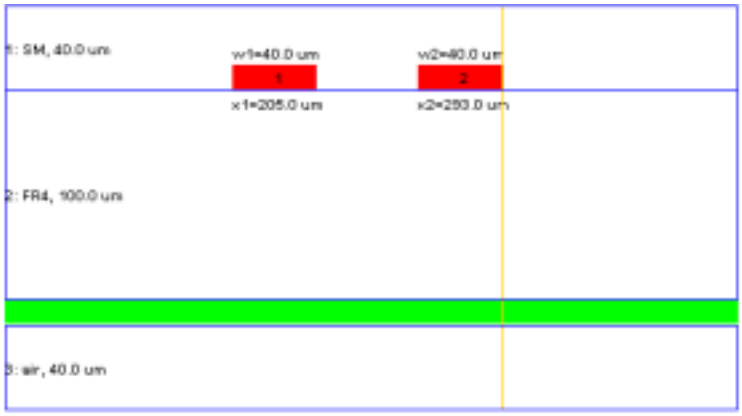

Figure 5.11: Coupled microstrips in a package layer.

Two coupled microstrips are laid in a PCB structure as shown in Figure 5.11. The trace widths are 100 um, with spacing of 140 um. The calculated impedance matrix is shown in Figure 5.12. This project file is under /examples/pkg_ustrip2.

Characteristic impedance in (Ohm), ignoring losses:
Even mode: 1.14140e+002, Common mode: 5.70699e+001
Odd mode: 5.02372e+001, Differential mode: 1.00474e+002

Figure 5.12: Impedance matrix of a pair of coupled microstrips in a package environment.

5.7 Coupling between Differential Eight Traces in a Package Structure

Figure 5.13: Eight traces on two layers with additional coupling through a gap in plane.

As shown in Figure 5.13, eight traces are laid in a package environment, with four on Layer 1 and four on Layer 3. Layer 2 is primarily a ground plane, but with a slot opening of size 70 um. The presence of the gap causes couplings between all traces. The calculated impedance matrix is shown in Figure 5.14. This project file is under /examples/pkg_xtk.

Characteristic impedance in (Ohm), ignoring losses:

6.72961e+001	1.68391e+001	2.77912e+000	-4.18276e-004	-1.39049e-001	-1.05650e-001	-1.47007e-001	-2.53448e-001
1.68391e+001	6.89056e+001	1.11845e+001	2.77912e+000	-1.19891e-001	4.37421e-001	3.69653e-001	-1.66221e-001
2.77912e+000	1.11845e+001	6.89056e+001	1.68391e+001	-1.66221e-001	3.69653e-001	4.37421e-001	-1.19891e-001
-4.18276e-004	2.77912e+000	1.68391e+001	6.72961e+001	-2.53448e-001	-1.47007e-001	-1.05650e-001	-1.39049e-001
-1.39049e-001	-1.19891e-001	-1.66221e-001	-2.53448e-001	5.60208e+001	1.14005e+001	2.63207e+000	1.68162e+000
-1.05650e-001	4.37421e-001	3.69653e-001	-1.47007e-001	1.14005e+001	5.69521e+001	7.31616e+000	2.63207e+000
-1.47007e-001	3.69653e-001	4.37421e-001	-1.05650e-001	2.63207e+000	7.31616e+000	5.69521e+001	1.14005e+001
-2.53448e-001	-1.66221e-001	-1.19891e-001	-1.39049e-001	1.68162e+000	2.63207e+000	1.14005e+001	5.60208e+001

Figure 5.14: Impedance matrix of eight coupled package traces.

5.8 Differential Coplanar Design in a Thin-Film Structure

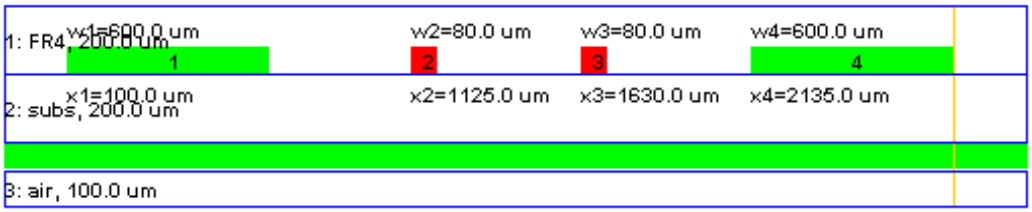

Figure 5.15: Differentially coupled co-planar waveguide structure on a thin-filem substrate.

On a thin-film substrate, a pair of differentially coupled coplanar lines are designed as shown in Figure 5.15. The width is 80 um, and spacing of 425 um. The distance between the outer edges of the differential pair and the ground planes are also 425 um. The calculated impedance matrix is shown in Figure 5.16. This project file is under /examples/tf_dcpw.

Characteristic impedance in (Ohm), ignoring losses:
Even mode: 5.18705e+001, Common mode: 2.59353e+001
Odd mode: 4.37641e+001, Differential mode: 8.75282e+001

Figure 5.16: Impedance matrix of a differentially coupled co-planar waveguide pair.

CHAPTER 5 — MANUSCRIPT

Part II

Theoretical and Technical Notes

— MANUSCRIPT

For advanced users, it is always beneficial to understand some the "under-the-hood" details of the tool in order to be an expert. The problems addressed by this tool fall into a special category of the so-called multi-conductor transmission-line (MTL) structure in the layered dielectric media. For a system to qualify to be a transmission-line structure, there need to be at least two metal pieces with uniform cross-sections. Electromagnetic (EM) waves can propagate along the metal lines. In particular, when the axial (or longitudinal) components of the EM fields are zero, the waves are in the so-called transverse electromagnetic (TEM) mode. Often, the axial components are not zero, but are much smaller than the transverse components, resulting in the so-called quasi-TEM mode. The analyses of the tool assume quasi-TEM modes for all EM waves supported by the traces being considered.

Theories and techniques of solving MTL system have been very mature [2], and widely used inside many CAD or CAE tools. Two of the most popular techniques are the finite element method (FEM) and the method of moment (MOM) formulated in the frequency domain. This tool is developed based on the MOM technique, which heavily relies on the evaluation of the Green's function in layered dielectric media. The following chapters cover only the MOM related techniques of solving the MTL problem.

Chapter 6

Multiconductor Transmission Line Theory

Assume that there are N_p planes, N_g traces connected to the ground (or GND in short) node that is always kept at zero potential ($\phi = 0$), and N signal traces. For the MTL system behave properly, it is necessary to have $N_p + N_g \geq 1$. In other words, there needs to be at least one conductor designated to be the reference conductor. Since the planes and the grounded traces are not the subjects of concern, only the voltages and current associated with the N signal traces are discussed in the MTL formulation.

6.1 Frequency-Domain MTL Equations

Denote

$$\mathbf{I} = \begin{bmatrix} I_1 & I_2 & \cdots & I_N \end{bmatrix}^T$$

$$\mathbf{V} = \begin{bmatrix} V_1 & V_2 & \cdots & V_N \end{bmatrix}^T$$

to be the arrays of currents and voltages on the N signal traces. Let spatial variable y to represent the position along the direction of wave propagation. In general, all $\mathbf{I}/\mathbf{V}$ components are functions of y. Introducing four matrices ($\mathbf{R}$, $\mathbf{L}$, $\mathbf{G}$, $\mathbf{C}$) of per-unit-length resistance, inductance, conductance, and capacitance quantities, the following matrix equations describe the MTL system:

$$\frac{d}{dz}\mathbf{V}(y) = -(\mathbf{R}+j\omega\mathbf{L})\mathbf{I}(y),$$

$$\frac{d}{dz}\mathbf{I}(y) = -(\mathbf{G}+j\omega\mathbf{C})\mathbf{V}(y),$$

where $\omega = 2\pi f$, is the angular frequency variable. A per-unit-length impedance matrix is defined as

$$\mathbf{Z} = \mathbf{R}+j\omega\mathbf{L},$$

and a per-unit-length admittance matrix is defined as

$$\mathbf{Y} = \mathbf{G}+j\omega\mathbf{C}.$$

Therefore, the system equations can also be written as

$$\begin{aligned} \frac{d}{dz}\mathbf{V}(y) &= -\mathbf{ZI}(y), \\ \frac{d}{dz}\mathbf{I}(y) &= -\mathbf{YV}(y). \end{aligned}$$

6.2 Characteristic Impedance Matrix

Denote matrix $\mathbf{T}_V$ that turns matrix $\mathbf{Z}$ into a diagonal form through a similarity transform. Likewise, denote matrix $\mathbf{T}_I$ that turns matrix $\mathbf{Y}$ into a diagonal form through another similarity transform. It can be shown that

$$(\mathbf{T}_I)^T = (\mathbf{T}_V)^{-1}.$$

Let

$$\mathbf{T} = \mathbf{T}_I,$$

then from the MTL equations, the following identity can be derived:

$$\mathbf{T}^{-1}(\mathbf{YZ})\mathbf{T} = \boldsymbol{\gamma}^2 = \begin{bmatrix} \gamma_1 & 0 & \cdots & 0 \\ 0 & \gamma_2 & \ddots & \vdots \\ \vdots & \ddots & \ddots & 0 \\ 0 & \cdots & 0 & \gamma_N \end{bmatrix}.$$

Defining the square-root of the matrix product as

$$\sqrt{\mathbf{YZ}} \equiv \mathbf{T}\boldsymbol{\gamma}\mathbf{T}^{-1}$$

which satisfies

$$(\sqrt{\mathbf{YZ}})^2 = \mathbf{T}\boldsymbol{\gamma}^2\mathbf{T}^{-1} = \mathbf{YZ}.$$

The characteristic impedance matrix is defined as

$$\mathbf{Z}_C \equiv \mathbf{Y}^{-1}\sqrt{\mathbf{YZ}} = \mathbf{Z}(\sqrt{\mathbf{YZ}})^{-1}.$$

When $N = 1$, for a single trace, the propagation constant and the characteristic impedance take the familiar forms of

$$\begin{aligned} \gamma &= \sqrt{YZ} = \sqrt{(R + j\omega L)(G + j\omega C)} \\ Z_C &= \sqrt{\frac{Z}{Y}} = \sqrt{\frac{R + j\omega L}{G + j\omega C}}. \end{aligned}$$

Chapter 7

Techniques of Finding the RLGC Parameters of MTL

The most important parameter is the per-unit-length capacitance matrix. Once the procedure of finding **C** is developed, the rest of the parameters can be derived.

Chapter 8

Methods used in Trace Analyzer

8.1 Green's Function in Layered Media

The scalar potential function $\phi(x, z)$ can be expressed in terms of the charge density $\sigma(x', z')$ and the 2D spatial Green's function $G^{\phi}(x, x'; z, z')$ by

$$\phi(x, z) = \int_C \sigma(x', z') G^{\phi}(x, x'; z, z') d\xi \tag{8.1}$$

where path C encompasses all boundaries of metal objects. The 2D spatial Green's function is derived from the 3D spectral Green's function $\tilde{G}(\gamma; z, z')$ by [6]

$$G^{\phi}(x, x'; z, z') = \frac{1}{2\pi} \int_{-\infty}^{\infty} \tilde{G}^{\phi}(\gamma, z, z') e^{j\gamma(x-x')} d\gamma. \tag{8.2}$$

The spectral Green's function satisfies

$$\left(\frac{\partial^2}{\partial z^2} + k_z^2 \right) \tilde{G}^{\phi}(x, x'; z, z') = -\delta(z - z').$$

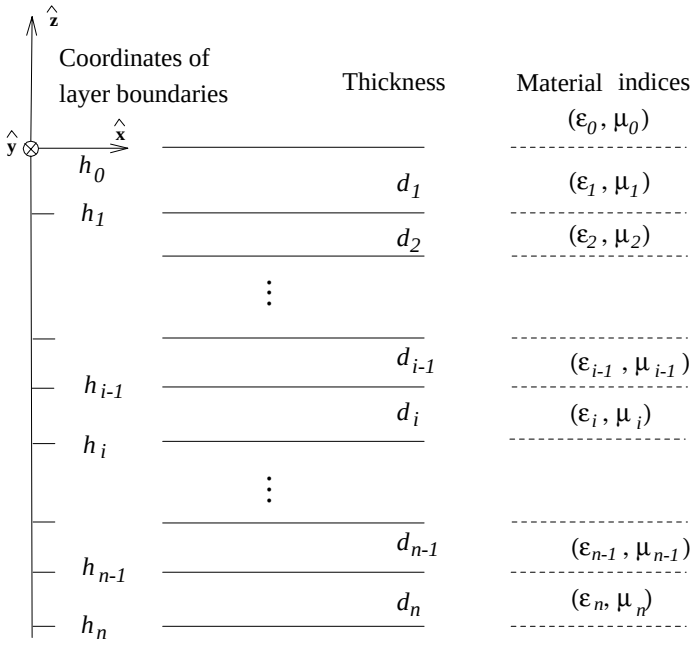

Figure 8.1: Description of dielectric layers with infinite lateral extent (in x, y directions). Either the top or the bottom side may be terminated by a perfect electric conductor (PEC).

Bookkeeping for a multi-layered structure

A general multi-layered dielectric stackup is comprised of a sequence of n dielectric slabs stacked along the vertical or z-direction. It is assumed that each dielectric slab has infinite extent in the lateral xy-plane to simplify the calculations. There are variations in the book-keeping methods for such structures: (1) The positive $\hat{z}$ can be defined either upward or downward; (2) The material indexing can be either increasing or decreasing along the $\hat{z}$ direction; (3) The global vertical reference location for $z = 0$ can be fixed within a particular layer or can be flexible. All three factors

affect the expressions of the spectral Green's functions. A scheme that is most suitable to the multilayered PCB/package design convention is adopted here and illustrated in Figure 8.1:

- The $+\hat{z}$ direction points upward;
- The material index starts from 0 and increases along the $-\hat{z}$ direction;
- The global $z = 0$ reference is flexible in all derivations of $\tilde{G}^{\phi}$. But eventually the $z = 0$ reference shall be chosen in computation. It is suggested that the $z = 0$ location be the boundary between the 0-th and the 1st materials, implying $h_0 = 0$.
- Then all boundaries between the neighboring slabs are given by

$$h_i = h_{i-1} - d_i \text{ for } i = 1..n \tag{8.3}$$

  where d_i is the thickness of the ith layer.

8.2 The spectral-domain Green's functions

The spectral Green's functions in simple layered-structures such as microstrip and stripline are well known [7, 8]. For structures involving three layers, the static Green's function can also be found in the literature [9]. All the necessary equations that can be applied to the derivation of spectral Green's functions in a general multilayered structure are given in Chew's book [10]. Chow et al. [11, 12] recognized that the spectral

Green's functions can be approximated by a series of complex images using the well-known Prony's method. One research group led by Aksun has devoted tremendous effort to the subject of computing the so-called closed-form spatial Green's functions in general layered media [13, 14, 15, 16, 17] where the key is the improvement of the Prony's method – a numerical technique called the generalized pencil of function (GPOF) first introduced by Hua [18, 19]. The spectral Green's functions $\tilde{G}^{\phi}$ were found in complete and efficient forms by Tsai [20]. Detailed steps suitable for computer implementation are given toward the derivation of the spectral Green's functions based on the information from all the above references.

8.2.1 Generalized Reflection Coefficients

The spectral Green's functions are expressed in terms of many coefficients which should be calculated first. Assume the frequency f and $\omega = 2\pi f$ is set. With iterations taken through $p, j = 1..n$ for the index of the field-point layer, the wave number in the p-th layer is

$$k_p = \omega\sqrt{\epsilon_p \mu_p}, \tag{8.4}$$

and the propagation constant along the z-direction can be defined by either

$$k_{zj} = \sqrt{k_j^2 - k_\rho^2} \tag{8.5}$$

or

$$\gamma_j = jk_{zj} = \sqrt{k_\rho^2 - k_j^2} \tag{8.6}$$

where

$$k_\rho^2 = k_x^2 + k_y^2 \tag{8.7}$$

is invariant with respect to index j due to the phase-matching boundary conditions [21]. In the above equations, j has been used as both an layer index and $\sqrt{-1}$. It is advantageous to use γ_j instead of k_{zj} to avoid confusion. The complex square-root operation is multi-valued [22]. Only the root for γ_j that is within the first quadrant (or k_{zj} within the fourth quadrant) is selected according to the Sommerfeld radiation condition [10]. In practice, the propagation constant γ_i value in the source layer (the ith) is calculated first, then the propagation constant in all other layers can be found by

$$\gamma_j = \sqrt{k_\rho^2 - k_j^2} = \sqrt{\gamma_p^2 + \omega^2(\epsilon_p\mu_p - \epsilon_j\mu_j)} \text{ for all } j \neq p. \tag{8.8}$$

Here, all $\gamma_j's$ are functions of $\{\omega, \gamma_p\}$.

The regular local reflection coefficients at an interface between two semi-infinite media with index $i = 1..n$ for all $R_{i+}^{TE,TM}$ and $i = 0..n$ for all $R_{i-}^{TE,TM}$ are

$$\begin{aligned} R_{i\pm}^{TE} &= 0, \text{ with a continuous half-space} \\ &= -1, \text{ with a PEC ground plane} \\ &= \frac{\gamma_i\mu_{i\mp1} - \gamma_{i\mp1}\mu_i}{\gamma_i\mu_{i\mp1} + \gamma_{i\mp1}\mu_i}, \text{ otherwise} \end{aligned} \tag{8.9}$$

and

$$\begin{aligned} R_{i\pm}^{TM} &= 0, \text{ with a continuous half-space} \\ &= 1, \text{ with a PEC ground plane} \\ &= \frac{\gamma_i \epsilon_{i\mp 1} - \gamma_{i\mp 1}\epsilon_i}{\gamma_i \epsilon_{i\mp 1} + \gamma_{i\mp 1}\epsilon_i}, \text{ otherwise.} \end{aligned} \tag{8.10}$$

The generalized reflection coefficient along the $+\hat{z}$ direction at $z = 0$ is

$$\tilde{R}_{1+}^{TE,TM} = R_{1+}^{TE,TM}, \tag{8.11}$$

then recursively for $i = 2..n$

$$\tilde{R}_{i+}^{TE,TM} = \frac{R_{i+}^{TE,TM} + \tilde{R}_{(i-1)+}^{TE,TM} e^{-2\gamma_{i-1}d_{i-1}}}{1 + R_{i+}^{TE,TM}\tilde{R}_{(i-1)+}^{TE,TM} e^{-2\gamma_{i-1}d_{i-1}}}. \tag{8.12}$$

The generalized reflection coefficient along the $-\hat{z}$ direction at $z = 0$ is

$$\tilde{R}_{n-}^{TE,TM} = R_{n-}^{TE,TM} \tag{8.13}$$

then recursively, for $i = (n-1)..0$

$$\tilde{R}_{i-}^{TE,TM} = \frac{R_{i-}^{TE,TM} + \tilde{R}_{(i+1)-}^{TE,TM} e^{-2\gamma_{i+1}d_{i+1}}}{1 + R_{i-}^{TE,TM}\tilde{R}_{(i+1)-}^{TE,TM} e^{-2\gamma_{i+1}d_{i+1}}}. \tag{8.14}$$

The local transmission coefficient at $z = 0$ is

$$\begin{aligned} S_{1+}^{TE,TM} &= 1 - R_{1+}^{TE,TM}, \text{ if it is used to calculate } G_x^{\phi} \\ &= 1 + R_{1+}^{TE,TM}, \text{ otherwise} \end{aligned} \tag{8.15}$$

then for $q = 2..n$

$$\begin{aligned} S_{q+}^{TE,TM} &= \frac{1 - R_{q+}^{TE,TM}}{1 - R_{(q-1)-}^{TE,TM} \tilde{R}_{(q-1)+}^{TE,TM} e^{-2\gamma_{q-1} d_{q-1}}} \text{ , if it is used to calculate } G_x^{\phi} \\ &= \frac{1 + R_{q+}^{TE,TM}}{1 - R_{(q-1)-}^{TE,TM} \tilde{R}_{(q-1)+}^{TE,TM} e^{-2\gamma_{q-1} d_{q-1}}}, \text{ otherwise.} \end{aligned} \tag{8.16}$$

For every fixed field layer index p, the generalized transmission coefficients for the varying source layer index $j = (p+1)..n$ are

$$\bar{T}_{TE,TM}^{(jp)^+} = S_{j+}^{TE,TM} \prod_{q=p+1}^{j-1} e^{-\gamma_q d_q} S_{q+}^{TE,TM}. \tag{8.17}$$

The running product is unity if the upper limit is smaller than the lower limit. Additionally, the $\tilde{M}$ factors are given by

$$\tilde{M}_i^{TE,TM} = \frac{1}{1 - \tilde{R}_{i+}^{TE,TM} \tilde{R}_{i-}^{TE,TM} e^{-2\gamma_i d_i}} \tag{8.18}$$

for $i = 1..n$.

8.2.2 Green's Functions for an Arbitrary Frequency

The Green's functions for the case where both the source and field points are in the p-th layer is

$$\begin{aligned}
\tilde{G}^{\phi(pp)} = & \frac{1}{2\gamma_p\epsilon_p}\{e^{-\gamma_p|z_f-z_s|} \\
& + \frac{\omega^2\epsilon_p\mu_p}{\omega^2\epsilon_p\mu_p+\gamma_p^2}\tilde{M}_p^{TE}[\tilde{R}_{p+}^{TE}e^{-\gamma_p(2h_{p-1}-z_f-z_s)} + \tilde{R}_{p-}^{TE}e^{-\gamma_p(z_f+z_s-2h_p)} \\
& + \tilde{R}_{p+}^{TE}\tilde{R}_{p-}^{TE}(e^{-\gamma_p(2d_p+z_f-z_s)} + e^{-\gamma_p(2d_p-z_f+z_s)})] \\
& - \frac{\gamma_p^2}{\omega^2\epsilon_p\mu_p+\gamma_p^2}\tilde{M}_p^{TM}[\tilde{R}_{p+}^{TM}e^{-\gamma_p(2h_{p-1}-z_f-z_s)} + \tilde{R}_{p-}^{TM}e^{-\gamma_p(z_f+z_s-2h_p)} \\
& - \tilde{R}_{p+}^{TM}\tilde{R}_{p-}^{TM}(e^{-\gamma_p(2d_p+z_f-z_s)} + e^{-\gamma_p(2d_p-z_f+z_s)})]\}. \qquad (8.19)
\end{aligned}$$

NOTE: The Green's functions used in the previous chapters do not include the factor of ϵ_p in $\tilde{G}^{\phi}$.

The Green's function take different forms for the case where the source point is in the j-th layer and the field point is in the p-th layer ($j \neq p$). By virtue of reciprocity [23] $\tilde{G}^{ij}(z_s, z_f) = \tilde{G}^{ji}(z_f, z_s)$, therefore, only the cases of $j = (p+1)..n$ need

to be discussed. Assume $j > p$, $z_f > z_s$, then

$$\tilde{G}^{\phi(pj)} = \frac{1}{2\gamma_j \epsilon_j (\omega^2 \epsilon_p \mu_p + \gamma_p^2)} \{ \omega^2 \epsilon_j \mu_j \bar{T}^{(jp)+} \tilde{M}_j^{TE}$$

$$\cdot [e^{-\gamma_j (h_{j-1} - z_s)} + \tilde{R}_{j-}^{TE} e^{\gamma_j (z_s + h_{j-1} - 2h_j)}]$$

$$\cdot [e^{-\gamma_j (z_f - h_p)} + \tilde{R}_{p+}^{TE} \, e^{-\gamma_p (2h_{p-1} - h_p - z_f)}]$$

$$+ \gamma_j^2 \bar{T}_{TM}^{(jp)+} \tilde{M}_j^{TM}$$

$$\cdot [e^{-\gamma_j (h_{j-1} - z_s)} - \tilde{R}_{j-}^{TM} e^{-\gamma_j (z_s + h_{j-1} - 2h_j)}]$$

$$[e^{-\gamma_p (z_f - h_p)} - \tilde{R}_{p+}^{TM} \, e^{-\gamma_p (2h_{p-1} - h_p - z_f)}] \; \}. \tag{8.20}$$

8.2.3 The Static Green's Functions

In multi-conductor transmission-line calculations, only the static Green's function is used. Although there is little difference between the general frequency-dependent Green's functions and the static Green's functions ($\omega = 0$) procedure-wise, when the spectral Green's functions are evaluated and fitted into a series of complex exponentials before using the Sommerfeld identity for the inverse Fourier transform, the expressions of the static Green's functions are simpler. In the static case,

$$\gamma_p = \gamma \tag{8.21}$$

is independent of the index p. For the case where both the source and field points are in the p-th layer, If all layers are non-magnetic, i.e., $\mu_i = \mu_0$ for all i's, then all $\tilde{R}^{TE} = 0$,

and

$$\tilde{G}^{\phi(pp)} = \frac{1}{2\gamma\epsilon_p}\{e^{-\gamma|z_f - z_s|}$$

$$-\tilde{M}_p^{TM}[\tilde{R}_{p+}^{TM} e^{-\gamma(2h_{p-1} - z_f - z_s)} + \tilde{R}_{p-}^{TM} e^{-\gamma(z_f + z_s - 2h_p)}$$

$$-\tilde{R}_{p+}^{TM}\tilde{R}_{p-}^{TM}(e^{-\gamma(2d_p + z_f - z_s)} + e^{-\gamma(2d_p - z_f + z_s)})]\}. \tag{8.22}$$

The Green's function for the case where the source point is in the j-th layer and the field point is in the p-th layer ($p \neq j$) with $j = (p+1)..n$ (or $j > p$) and $z_f > z_s$ is, assuming all layers are non-magnetic,

$$\tilde{G}^{\phi(pj)} = \frac{1}{2\gamma\epsilon_j}\bar{T}_{TM}^{(jp)+}\tilde{M}_j^{TM}$$

$$[e^{-\gamma(h_{j-1} - z_s)} - \tilde{R}_{j-}^{TM} e^{-\gamma(z_s + h_{j-1} - 2h_j)}]$$

$$[e^{-\gamma(z_f - h_p)} - \tilde{R}_{p+}^{TM}\, e^{-\gamma(2h_{p-1} - h_p - z_f)}]\ . \tag{8.23}$$

8.2.4 Complex Image Technique

It is possible to approximate a general spectral Green's function described above in terms of a sum of complex exponentials [11][18]

$$\tilde{G}^{\phi}(\gamma; z_s, z_f) = \frac{1}{2\gamma}\sum_{i=1}^{M}\alpha_i e^{-\gamma_j a_i} \tag{8.24}$$

where γ_j is for the source layer. The spatial domain is then determined by [6] following Eqn. (8.2), or

$$G^{\phi}(x, x'; z_s, z_f) = \frac{1}{2\pi}\int_{-\infty}^{\infty} d\gamma \tilde{G}^{\phi}(\gamma; z_s, z_f) e^{j\gamma(x - x')}.$$

Eqn. (**??**) can be simplified, using Eqn. (8.24), as

$$G^{\phi}(x,x';z_s,z_f) = \frac{1}{2\pi\epsilon_s}\sum_{i=1}^{M}\alpha_i \ln\frac{1}{\sqrt{\left|\frac{x-x'}{X_0}\right|^2+\left(\frac{a_i}{X_0}\right)^2}}, \tag{8.25}$$

where

$$X_0 = 1 \text{ meter}.$$

The constants $a_i's$ and $\alpha_i's$ constitute the so-called complex images. The term in $G^{\phi}(x,x';z_s,z_f)$ with $a_i = 0$ is identified as the "direct term" which represents a singularity when $|x-x'| = 0$. Therefore, Eqn. (8.25) can be written as

$$G^{\phi}(x,x';z_s,z_f) = G^{\phi}_{direct}(x,x';z_s,z_f) + G^{\phi}_{indirect}(x,x';z_s,z_f)$$

where

$$\begin{aligned} G^{\phi}_{direct}(x,x';z_s,z_f) &= \frac{1}{2\pi\epsilon_s}\alpha_D \ln\frac{1}{\left|\frac{x-x'}{X_0}\right|}, \\ G^{\phi}_{indirect}(x,x';z_s,z_f) &= \frac{1}{2\pi\epsilon_s}\sum_{i=1,a_i\neq 0}^{M}\alpha_i \ln\frac{1}{\sqrt{\left|\frac{x-x'}{X_0}\right|^2+\left(\frac{a_i}{X_0}\right)^2}}. \end{aligned}$$

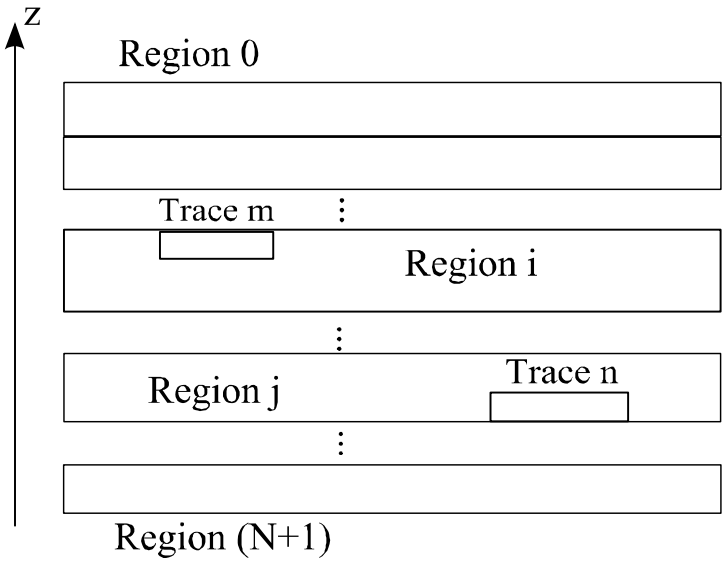

Figure 8.2: Traces in a multi-layered dielectric media.

8.3 Method of Moment Formulation for Computing the C Matrix

As shown in Figure 8.2, two arbitrary traces indexed m and n are drawn. Each trace characterized by its width and thickness is modeled by a rectangular metal shell (shell has zero thickness). All edges of the rectangle of a typical trace, say Trace m, are divided into small segments, as illustrated by Figure 8.3. Line segments are the fundamental constructs that are interacting with each other.It is known that the charge density on a typical edge is not uniformly distributed. As a matter of fact, the charge density

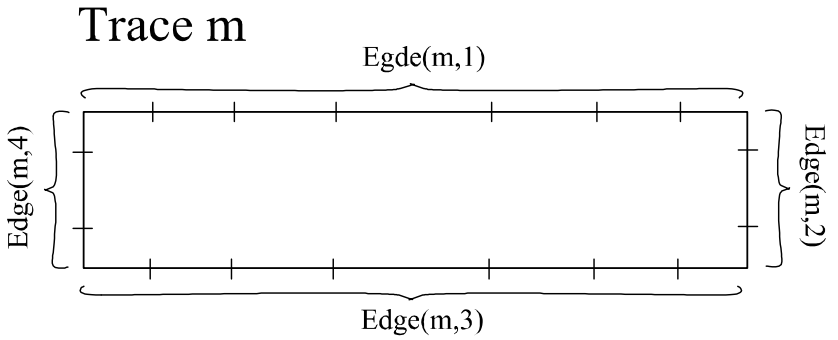

Figure 8.3: Edges of a typical trace are divided into line segments.

function takes the form of

$$\sigma(\xi) = \frac{P_0}{\sqrt{1-(2\xi/w)^2}} \tag{8.26}$$

assuming a local coordinate system shown in Figure 8.4, where P_0 is a constant. It is suggested by [24] that the edge should not be evenly divided. Instead, the center positions of the segments follow the abscissas of a Chebyshev-Gauss quadrature. Specifically, in the local coordinates (in ξ), these points are calculated by

$$\xi_k = \frac{w}{2}\cos(\frac{2k-1}{2N_\xi}\pi) \text{ for } k = 1, 2, .., N_\xi \tag{8.27}$$

with N_ξ being the number of segments along an edge. The benefit of this particular way of dividing edges into segments naturally account for the charge density distribution characterized by Eqn. (8.26) if each segment has the same amount of total charge.

With method of moment (MOM), all metal boundaries are divided into segments. Treating each segment as a basic unit, a system of segments are formed. The integral of Eqn. (8.1) is transformed to a set of linear equations. The potential associ-

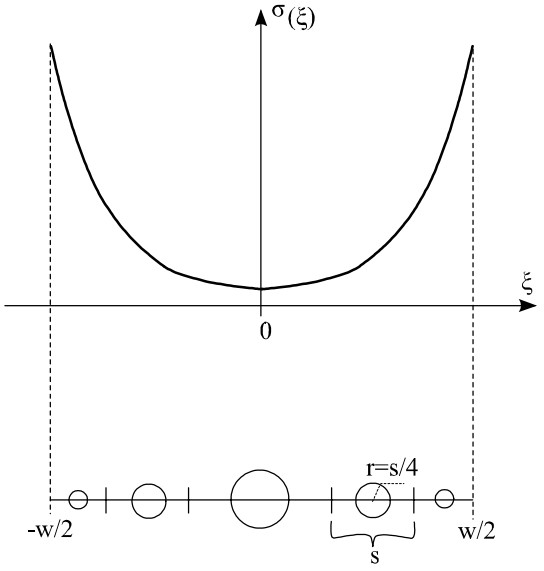

Figure 8.4: One typical edge of a trace.

ated with Segment-m is related with the charge of at Segment-n by

$$\phi_m = K_{mn}\sigma_n \tag{8.28}$$

where the interaction terms (inverse capacitance in unit) can be computed with [24]

$$K_{mn} = \begin{cases} G^{\phi}_{direct}(x_m, x'_n; z_s, z_f) + G^{\phi}_{indirect}(x_m, x'_n; z_s, z_f) \text{ if } m \neq n \\ G^{\phi}_{direct}(0, r_m; z_s, z_f) + G^{\phi}_{indirect}(x_m, x'_n; z_s, z_f) \text{ if } m = n \end{cases}$$

where the quantity r_m is a "pipe radius" corresponding to each segment along an edge, as shown in Figure 8.4. Actually, $r'_m s$ can be immediately evaluated, once the center coordinates are calculated with Eqn. (8.27), by

$$r_m = \frac{w}{8}\frac{1}{\prod_{i=1, i\neq m}\frac{|\xi_m - \xi_i|}{w/2}},$$

noticing that the coordinates can be more efficiently stored in dimension-less form of $\xi_i/(w/2)$.

The matrix representation of Eqn. (8.28) is

$$[\mathbf{\Phi}] = [\mathbf{K}][\boldsymbol{\sigma}],$$

which can be inverted to have

$$[\boldsymbol{\sigma}] = [\mathbf{K}]^{-1}[\mathbf{\Phi}].$$

Denote

$$\mathbf{C}_{seg} = [\mathbf{K}]^{-1}, \tag{8.29}$$

which is the segment level capacitance matrix. Suppose that there are M traces, due to the fact that each trace has the same potential for all its constituent segments. The raw capacitance matrix of Eqn. (8.29) can be reduced to a $M \times M$ matrix $\mathbf{C}$ using the following algorithm:

for each segment i

{

determining trace index $m(i)$;

for each segment j

{

determining trace index $n(j)$;

$C_{mn} += C_{raw}(i, j)$;

}

}

It is assumed that the **C** matrix elements were initially set to zeros. The $m(i)$ and $n(j)$ are the mapping from the segment index to the trace index.

8.4 Computing the L Matrix

Once the procedure of computing $\mathbf{C}$ matrix is established, a special capacitance matrix, $\mathbf{C_0}$, associated with the same set of traces with dielectric layers removed (left with vacuum), can be easily computed. The inductance matrix for a non-magnetic media is given by [25]

$$\mathbf{L} = \mu_0 \epsilon_0 \mathbf{C}_0^{-1}.$$

When there are magnetic materials in some layers, the inductance matrix can be determined by [26]

$$\mathbf{L} = \mu_0 \epsilon_0 \mathbf{C}_{R,0}^{-1}.$$

where the $\mathbf{C}_{R,0}$ matrix is computed by assigning the relative dielectric constant of each magnetic layer as

$$\epsilon_r = \mu_r^{-1}.$$

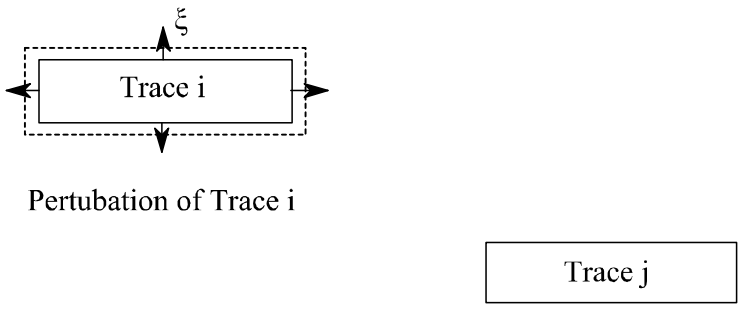

Figure 8.5: Scheme of computing skin resistance matrix.

8.5 Computing the R Matrix

The resistance matrix can be broken into two parts: $\mathbf{R_0}$ of DC resistance, and $\mathbf{R}_s$ caused by the skin effect. Assuming σ to be the conductivity of the trace metal, the terms of $\mathbf{R_0}$ are simply given by Ohm's law as

$$R_{0,ij} = \begin{cases} \frac{1}{\sigma w_i t_i}, & i = j \\ 0 & i \neq j \end{cases}$$

where w_i and t_i are the width and thickness of Trace i, respectively.The terms of skin resistance calculation are computed by the Weeler's rule [6] by perturbing Trace i (expanding its surface outward by a distance of $\Delta\xi$ along the surface normal directions) and compute the inductance matrices before and after the perturbation:

$$R_{s,ij} = -\sqrt{\frac{\pi f}{\mu\sigma}} \frac{L_{ij}^{after} - L_{ij}^{before}}{\Delta\xi}.$$

8.6 Computing the G Matrix

The conductance matrix consists of two parts, i.e.,

$$\mathbf{G} = \mathbf{G_0} + \mathbf{G}_d$$

where $\mathbf{G}_d$ is caused by the dielectric loss, and $\mathbf{G_0}$ contains leakages by other mechanisms.

The dielectric-based conductance matrix can be obtained by using the complex permittivity values for each dielectric layer

$$\epsilon = \epsilon_r(1 - j\tan\delta).$$

Going through the complex-valued matrix algebra, the resultant capacitance matrix, $\hat{\mathbf{C}}$, is also complex-valued. Then splitting the real and imaginary parts, with

$$\mathbf{C} = \mathrm{Re}\{\hat{\mathbf{C}}\}$$

and the conductance matrix is simply

$$\mathbf{G}_d = -\omega\,\mathrm{Im}\{\hat{\mathbf{C}}\}.$$

Chapter 9

Appendix

9.1 Layer Stackup File Format

User can specify the unit in the z-direction by a statement in form of

Unit unit_name

where unit_name can be one of the followings: {in, cm, mm, mil, um, nm}.

All materials used in a specific layer stackup have to be defined. A material definition is in form of

material material_name

type = conductor or insulator

er = value

tand = value

mr = value

sigma = value

;

where

- material_name: Any name. But, it has to be in one word
- type: either "conductor" or "insulator"
- er: relative permittivity (dielectric constant)
- tanD: loss tangent
- mr: relative permeability
- sigma: conductivity in (S/m). It is important only for conductor, may use 0 for insulator

Then, the stackup file contains several interleaved dielectric and metal layer definition statements.

A dielectric layer is specified by

layer material_name

thickness = value

;

where material_name should be among the defined dielectric material names. thickness is a numerical value measured by the z unit.

A metal layer is specified by

layer material_name

index = metal_layer_index

thickness = value

under_cut = 0.0

trace_over_boundary = yes_or_no

 # between dielectric Layers n and (n+1)

z_offset = 0.0

;

where material_name should be among the defined conductor material names. metal_layer_index is an integer value (The top layer has index 1). thickness is a numerical value measured by the z unit. yes_or_no for the "trace_over_boundary" attribute can be "yes" if the trace bottom side coincide with the dielectric layer boundary, or "no" if the trace top side align with the dielectric layer boundary. If the metal layer is a plane, it is represented by both "trace_over_boundary=yes", and "trace_over_boundary=no".

9.1.1 Example

 # Tech file content

 # generated by EE Circle TraceAnalyzer

 # on 8-3-2007 at 2:38

 # Unit

Unit um

```
# BEGIN material Er_3.25
material Er_3.25
 type = insulator
 er = 3.25
 tand = 0.02
 mr = 1.0
 sigma = 0.0
 ;
# END material Er_3.25
# BEGIN material Copper
material Copper
 type = conductor
 er = 1.0
 tand = 0.0
 mr = 1.0
 sigma = 7.0E7
 ;
# END material Copper
# BEGIN material air
material air
 type = insulator
```

```
 er = 1.0
 tand = 0.0
 mr = 1.0
 sigma = 0.0
 ;
# END material air
# BEGIN material FR4
material FR4
 type = insulator
 er = 4.2
 tand = 0.02
 mr = 1.0
 sigma = 0.0
 ;
# END material FR4
# 1: The 1-th dielectric layer
 layer air
 thickness = 10.0
 ;
# 2: The 1-th metal layer
 layer Copper
```

index = 1

thickness = 5.0

under_cut = 0.0

 # constructed with entire_plane

trace_over_boundary = yes

trace_over_boundary = no

 # between dielctric Layers 1 and 2

z_offset = 0.0

;

 # 3: The 2-th dielectric layer

layer Er_3.25

thickness = 13.4

;

 # 4: The 2-th metal layer

layer Copper

index = 2

thickness = 1.4

under_cut = 0.0

trace_over_boundary = yes

 # between dielctric Layers 2 and 3

z_offset = 0.0

;

 # 5: The 3-th dielectric layer

layer Er_3.25

thickness = 12.0

;

 # 6: The 3-th metal layer

layer Copper

index = 3

thickness = 5.0

under_cut = 0.0

 # constructed with entire_plane

trace_over_boundary = yes

trace_over_boundary = no

 # between dielctric Layers 3 and 4

z_offset = 0.0

;

 # 7: The 4-th dielectric layer

layer air

thickness = 10.0

;

9.2 Trace Definition File Format

User can specify the unit in the x-direction by a statement in form of

Unit unit_name

where unit_name can be one of the followings: {in, cm, mm, mil, um, nm}.

Next, the total number of traces is specified by a statement in form of

Num number_of_traces

Then, each trace is specified by

Trace metal_layer_index x_left width s_or_g;

where

- metal_layer_index: index of the metal layer
- x_left: x-coordinate of the left edge of the trace
- width: trace width
- s_or_g: use "g" if the trace is grounded. "s" for regular signal trace

9.2.1 Example

 # Trace file

 # generated by EE Circle Trace Analyzer

 # on 8-3-2007 at 2:42

 # Unit

Unit um

 # Number of metal layers

Num 2

 # Each line format: Trace layer_index x_coord width s/g

Trace 2 10.0 11.7 s;

Trace 2 28.1 11.7 s;

9.3 Using RLGC Data in ADS

Using the bench mark case of Section 4.2, suppose a file named "ms2.ads" is generated by Trace Analyzer using the "Export RLGC for ADS" menu. This file should be copied into the data subdirectory of the ADS project.

The content of the ADS-RLGC file is listed below:

BEGIN DSCR(RLGC)

! C[i][j]/eps0 L[i][j]/mu0 Rdc[i][j] Rhf[i][j]/sqrt(f_GHz) G[i][j]/omega*eps0

% C(real) L(real) Rdc(real) Rhf(real) G(real)

13.81562 0.25464 0.00000 0.02510 0.02874

-2.50049 0.08515 0.00000 0.00666 -0.03986

-2.50049 0.08515 0.00000 0.00666 -0.03986

13.81562 0.25464 0.00000 0.02510 0.02874

END

If the ADS version comes with a license for the "SPICE Translator" tool, then it might be possible to use even the HSPICE W-element model file directly. For users of ADS without the "SPICE Translator" option, there is a work-round to import RLGC file with the following procedure (the example given below was tested on version 2003c):

In the schematic editor, switch the design palate to "TLines-Multilayer", choose a "Mlctl_v" element with the matching topology as defined in TraceAnalyzer. In this example, a coupled two line component ML2CTL_V should be selected. Mean-

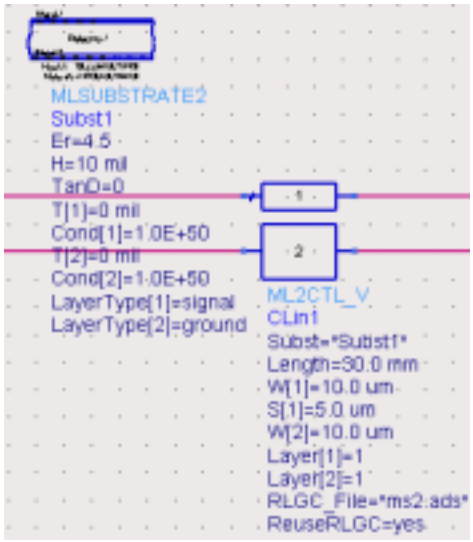

Figure 9.1: Using RLGC data inside an ADS design.

while, a substrate component, say, MLSUBSTRATE2 or any other substrate, is selected in order to have a valid ADS schematic design. Double click on the ML2CTL_V component, to set the following fields correctly:

- Length=30.0 mm
- RLGC File="ms2.ads"
- ReuseRLGC=yes

Other parameters are left untouched since they will not affect the behavior of the 4-port structure. It is important to know that the file was located inside the data subdirectory under the current ADS project. Also, by choosing "ReuseRLGC=yes", all the geometry and layer definitions will be ignored. Obviously, the length parameter

can be adjusted by the user to reflect the desired physical length.

Remark 2 be careful with the "ReuseRLGC" field. If it is accidentally set to "no", then the file "ms2.ads" will be overwritten by ADS in the next simulation, the file content will correlate to the geometry and layer parameters specified by the ML2CTL_V and MLSUBSTRATE2 components.

9.3.1 Time-Domain Verification of RLGC Parameters Generated by TraceAnalyzer in ADS

According to Trace Analyzer, the major characteristics of the coupled microstrip traces are:

Characteristic impedance in (Ohm), ignoring losses:

Even mode: 6.52991e+001, Common mode: 3.26495e+001

Odd mode: 3.84061e+001, Differential mode: 7.68122e+001

per-unit-length delay in (s/m), ignoring losses:

Mode1: 5.54575e-009

Mode2: 6.53898e-009

Now, the differential and common mode parameters with ADS transient simulations are shown in the figure below.

Marker m1 indicates the common-mode impedance of 32.562 (3.26495e+001 by Trace Analyzer). Marker m2 indicates the differential-mode impedance of 76.714

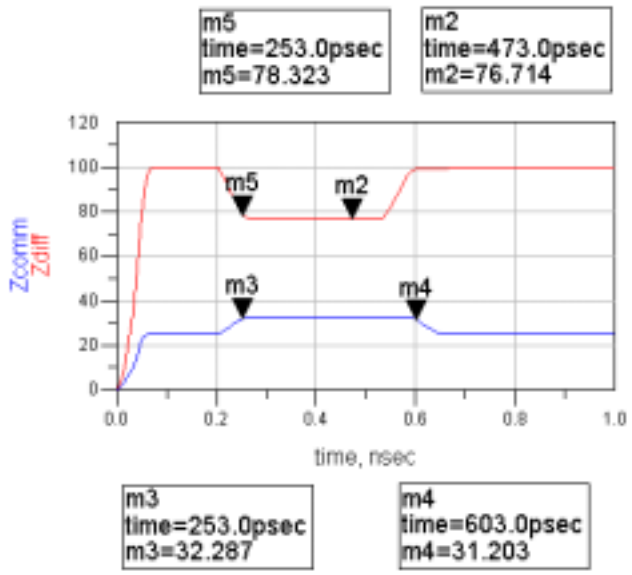

Figure 9.2: Time-domain verification of using RLGC data inside ADS.

(7.68122e+001 by Trace Analyzer)

The timing difference between markers m3 and m4 is 350 ps. For length of 30 mm and per-unit-length delay of 5.54575e-009 s/m (common-mode) calculated by Trace Analyzer, the total delay should be 2*0.03*5.54575e-009=3.32745e-10=332.7 ps, which is comparable to the Trace Analyzer result. Since there is a non-zero rise-time used in the transient simulation, the boundary of start and end points corresponding to the transmission-line terminals are somewhat difficult to determine.

Bibliography

[1] Brian C. Wadell, Transmission Line Design Handbook, Artech House, Boston, 1991.

[2] Clayton R. Paul, Analysis of Multiconductor Transmission Lines, Wiley Interscience, 1994.

[3] E. Recht and S. Shiran, "A simple model for characteristic impedance of wide microstrip lines for flexible pcb," in EEE EMC Symposium, 2000, pp. 1010–1014.

[4] Antonije R. Djordjevic, Miodrag B. Bazdar, Tapan K. Sarkar, and Roger F. Harrington, LINPAR manual, Artech House, 1999.

[5] Jr Daniel G. Swanson and Wolfgang J. R. Hoefer, Microwave Circuit Modeling using Electromagnetic Field Simulation, Artech House, 2003.

[6] Joaquin Bernal, Francisco Medina, and Manuel Horno, "Quick quasi-tem analysis of multiconductor transmission lines with rectangular cross section," IEEE Trans. Microw. Theory Tech., vol. 45, no. 9, pp. 1619 – 1626, Sept. 1997.

[7] T. Kitazawa and R. Mittra, "Analysis od asymptotic coupled striplines," IEEE Transactions on Microwave Theory and Techniques, vol. 33, pp. 643–646, 1985.

[8] W. J. Getsinger, "Dispersion of parrallel-coupled microstrip," IEEE Transactions on Microwave Theory and Techniques, vol. 21, pp. 144–145, 1973.

[9] K. J. Scott, "Efficient image theory for electromagnetic field modelling in PCB," Phillips Journal of Research, vol. 48, no. 1–2, pp. 37–61, 1994.

[10] Weng Cho Chew, Waves and Fields in Inhomogeneous Media, IEEE Press, New Jersey, 1995.

[11] Y. L. Chow, J. J. Yang, D. G. Fang, and G. E. Howard, "A closed-form spatical Green's function for the thick microstrip substrate," IEEE Transactions on Microwave Theory and Techniques, vol. 39, pp. 588–592, no. 3, March 1991.

[12] Read M. Shubair and Y. L. Chow, "Efficient computation of periodic Green's function in layered dielectric media," IEEE Transactions on Microwave Theory and Techniques, vol. 41, pp. 498–502, no. 3, March 1993.

[13] Gülbin Dural and M. I. Aksun, "Closed-form Green's functions for general sources and stratified media," IEEE Transactions on Microwave Theory and Techniques, vol. 43, pp. 1545–1552, no. 7, July 1995.

[14] M. Irsadi Askun and Gulbin Dural, "Closed-form Green's functions of HED, HMD, VED and VMD for multilayer media," Proceedings of IEEE Antennas and Prop-

agations Society International Symposium, Ann Arbor, MI, USA, pp. 354–357, 28 June – 2 July, 1993.

[15] M. I. Askun, "A robust approach for the derivation of closed-form Green's functions," IEEE Transactions on Microwave Theory and Techniques, vol. 44, pp. 651–658, no. 5, May, 1996.

[16] Lale Alatan, M. I. Aksun, Karthikeyan Mahadevan, and M. Tuncay Birand, "Analytical evaluation of the MoM matrix elements," IEEE Transactions on Microwave Theory and Techniques, vol. 44, pp. 519–525, no. 4, April 1996.

[17] Noyan Kinaman and M. I. Askun, "Efficient use of closed-form Green's functions for the analysis of planar geometries with vertical connections," IEEE Transactions on Microwave Theory and Techniques, vol. 45, pp. 593–603, no. 5, May 1997.

[18] YingBo Hua and Tapan K. Sarkar, "Generalized pencil-of-function method for extracting poles of an EM system from its transient response," IEEE Transactions on Antennas and Propagation, vol. 37, pp. 229–234, no. 2, February 1989.

[19] T. K. Sarkar and Odilon Pereira, "Using the matrix pencil method to estimate the parameters of a sum of complex exponentials," IEEE Antennas and Propagation magazine, vol. 37, no. 1, pp. 48–55, February 1995.

[20] Ming-Ju Tsai, Franco De Flaviis, Owen Fordham, and Nicolaos G. Alexopoulos, "Modeling planar arbitrary shaped microstrip elements in multilayered media,"

IEEE Transactions on Microwave Theory and Techniques, vol. 45, pp. 330–337, no. 3, March 1997.

[21] David M. Pozar, Microwave Engineering, Addison Wesley, New York, 1990.

[22] James Ward Brown and Ruel V. Churchill, Complex Variable and Applications, McGraw-Hill, New York, 1996.

[23] Constantine A. Balanis, Advanced Engineering Electromagnetics, John Wiley, New York, 1989.

[24] Gregory E. Howard, Jian Jun Yang, and Y. Leonard Chow, "A multipipe model of general strip transmission lines for rapid convergence of integral equation singularities," IEEE Trans. Microw. Theory Tech., vol. 40, no. 4, pp. 628 – 636, 1992.

[25] Cao Wei, R.F. Harrington, J. R. Mautz, and T.K. Sarkar, "Multiconductor transmission lines in multilayered dielectric media," IEEE Trans. Microw. Theory Tech., vol. 32, no. 4, pp. 439 – 450, 1984.

[26] J. R. Mautz, R. F. Harrington, and C. G. Hsu, "The inductance matrix of a multiconductor transmission line in multiple magnetic media," IEEE Trans. Microw. Theory Tech., vol. 36, no. 8, pp. 1293–1295, 1988.